Crystal-like growth of metal oxide/CNT composite with electroplated "seed"

W. J. Kim*, E. Y. Jang*, D. K. Seo*, T. J. Kang*, K. C. Jin**, D. H. Jeong** and Y. H. Kim*

* School of Mechanical and Aerospace Engineering and the Institute of Advanced Aerospace Technology, Seoul National University, San 56-1, Sillim-dong, Kwanak-gu, Seoul 151-742, Korea,
**Department of Chemistry Education, Seoul National University, San 56-1, Sillim-dong, Kwanak-gu, Seoul 151-742, Korea

yongkim@snu.ac.kr

ABSTRACT

A fabrication technique is developed for the preparation of metal oxide/CNT composites. An essential feature of the technique lies in the use of non-aqueous electrolyte in place of the usual aqueous electrolyte, which ensures well-dispersed CNTs without surfactants. After a "seed" is formed by electroplating on the anode, the seed is simply pulled up at a certain speed to grow one-dimensional CNT composite structure. The technique is able to distribute uniformly metal oxide and has high weight fraction of CNT in the composite structure. Moreover, the conductivity of the composite is much higher than those of CNT fibers fabricated with polymer because tungsten oxide plays a role of electron acceptor and current-induced thermal excitation recovers the crystalline of CNT.

Keywords: metal oxide/CNT composite, crystal-like growth, CNT-dispersed non-aqueous electrolyte, electroplating, dip-coating.

1. INTRODUCTION

Carbon nanotubes (CNTs) have extraordinary mechanical, chemical and electrical properties. One way of exploiting these excellent properties is to produce composite materials of metal, metal oxide, and ceramic with CNT. It has already been shown that CNT is an excellent reinforcement material for polymer/ceramic-based CNT[1-5] and metal/CNT composites[6-9]. Recent interest in metal or metal oxide/CNT composites stems from their utilization as an emitter in field emission display (FED), a thermal interface material, super capacitor, and interconnects in ultra-large scale integrated circuits[10-19]. Metal or metal-oxide/CNT composites have been prepared mostly by electroplating technique[11-18] and in particular, aqueous electrolyte has been used for the electroplating. It is difficult to disperse carbon nanotubes uniformly in aqueous electrolyte without surfactants because of strong van der Waals interactions among them due to their hydrophobic nature. As a result, agglomerated CNTs form in the composite matrix and the composite properties become much worse than expected.

In this work, we utilize a non-aqueous electrolyte in place of an aqueous electrolyte in preparing a metal oxide/CNT composite. The non-aqueous electrolyte, which is sodium tungstate dehydrate ($Na_2WO_4 \cdot 2H_2O$, STD) dissolved in an organic solvent of *N,N*- dimethylformamide (DMF), readily dissolves acid-treated single-walled carbon nanotubes (SWNTs), resulting in a very stable CNT colloidal solution. The good dispersion of CNT that is made possible with the use of non-aqueous electrolyte ensures well dispersed CNTs in the prepared composite. We expect the CNT-dispersed non-aqueous electrolyte is able to contribute to the development of fabrication technique for metal oxide/CNT composite which has various dimensional structures. However, previous reports of metal oxide/CNT composite were narrowly concentrated in the thin film structure. Unfortunately one-dimensional metal oxide/CNT composite has not been reported yet, because homogenously dispersed CNT colloidal solution is essential prerequisite for forming continuous one-dimensional structure. We successfully obtained the macroscopic one-dimensional tungsten oxide/CNT composite fiber used by electroplating and dip-coating from the CNT-dispersed non-aqueous electrolyte.

In this fabrication of the tungsten oxide/CNT composite, the tungsten oxide intermixed with CNTs is electroplated on the tungsten tip, which acts as a "seed" for further growth of the composite. Once the seed is formed, it is simply pulled upward at a certain speed with the bias still on, creating a neck at the end of the seed, and then a small but enlarged cylindrical ingot forms at the neck in a way similar to the Czochralski crystal growth[20] that is typically used for the growth of silicon and III-V compound semiconductors. Although the structure of the grown ingot is not like that of a crystal, the CNTs in the grown ingot is well aligned in the direction of growth, as shown later. It is for this reason that the process might be called crystal-like growth of CNT composite.

2. EXPERIMENTAL DETAILS

Shown in Fig.1 is a schematic of the procedure involved in the fabrication of metal-oxide/CNT composite with non-aqueous electrolyte. The bottom frames show actual optical pictures of the fabrication steps. As shown in Fig. 1(a), a sharpened tungsten tip with a radius of curvature of 250nm is immersed into the electrolyte solution, which is CNT and

STD dissolved in DMF solvent for the WO_4/CNT composite being fabricated. In the schematic, the red and blue dots are WO_4^{-2} ions and reduced WO_4, respectively, and dark straight lines represent CNTs. Upon applying bias to the tungsten anode with the container bottom grounded, negatively charged CNTs that are acid-treated gather around the anode along with the WO_4^{-2} ions. The darker black color in the bottom frame of Fig. 1(b) clearly shows CNTs densely gathered around the electrode. After electroplating for 5 minutes, the electrode is pulled up as shown in Fig. 1(c) at a speed of 0.3 mm/min with the solution of CNTs and WO_4^{-2} attached to the tungsten tip. The bias is still on during the pulling. The high density of CNT in the tail column attached to the electrode is also apparent from the color in the bottom frame. After the desired length of the macroscopic one-dimensional CNT is reached, the electrode is quickly pulled up to complete the electroplating, as shown in Fig. 1(d). During and after the electroplating, the solvent in the exposed column of solution evaporates, leading eventually to the formation of the macroscopic one-dimensional CNT structure. The resulting structure is an interwoven network of aligned CNTs with WO_4 acting as binder and, as a result, the structure is mechanically strong. Note in this regard that the atomic ratio of carbon in the composite is close to 92%, as revealed later. Therefore, the WO_4/CNT composite contains only a small amount of WO_4 . It is also noted here that the pulling of the liquid column as shown in Fig. 1 was not possible in the absence of sodium tungstate dihydrates.

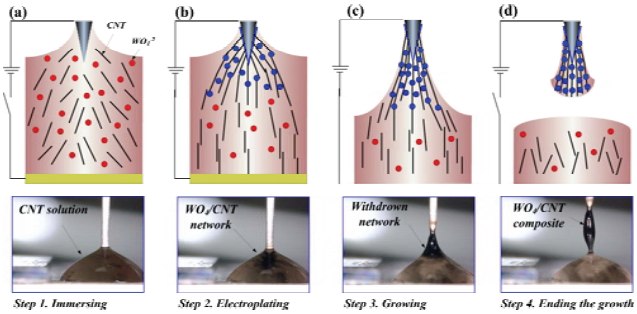

Figure 1. Schematic of the procedure for fabricating one-dimensional WO_4/CNT composite structure by crystal-like growth

3. RESULTS AND DISSUSSION

The length of the macroscopic one-dimensional CNT structure is entirely determined by the pulling time of the liquid column when the pulling speed is fixed, the length being longer for longer pulling time. The diameter of the one-dimensional structure can be varied by controlling the electroplating current. Shown in Fig. 2 is the structure diameter plotted with respect to the current. Various currents of 2 nA, 10 μA, 100 μA, 1 mA and 3 mA are applied for the samples numbered 1 through 5, respectively. The diameter increases with increasing current. The plot shows that the diameter increases almost linearly with logarithmic current. Varying the current implies adjusting the voltage, and therefore, a higher current indicates a higher bias applied. A higher bias draws more CNTs to the vicinity of the tungsten tip, which results in a larger diameter.

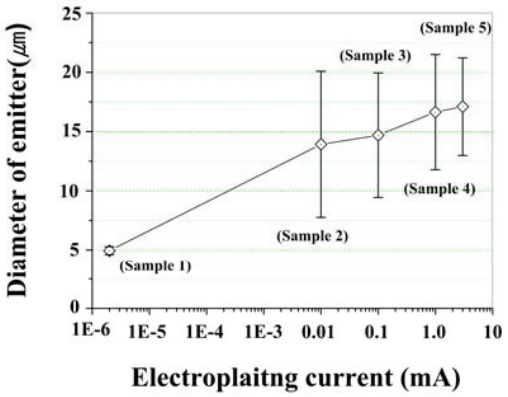

Figure 2. Diameter of WO_4/CNT composite vs. electroplating current.

An example of WO_4/CNT composite fabricated according to the procedure in Fig. 1 is shown in Fig. 3(a). The macroscopic one-dimensional CNT structure is 2.5 mm in length and 14 μm in diameter that was fabricated at a current of 1 mA with the pulling time of 10 minutes. The magnified scanning electron microscopy (SEM) image of the structure in Fig. 3(b,c) reveals the outside texture that appears to be cylindrical cords bound together in the direction of growth, which are somewhat interwoven. The alignment is a result of the surface tension of the solution exerted on WO_4/CNT composite network that was generated by electroplating and upward movement of the electrode [26, 27]. It is noted in this regard that the contact angle of the meniscus with the tungsten tip is acute as verified in our experiment with digital snapshots. The surface tension and the mass of the composite network below the solution surface act to generate vertical stress, which leads to the alignment of CNTs. The cross section of the composite was examined by tearing the composite off the tungsten tip, which is shown in Fig. 3(d) where tungsten tip is visible through the hole. The thickness of the composite on the tungsten tip was estimated to be about 5 μm. An examination of the inner surface of the delaminated composite that is shown in Fig. 3(e) reveals that the CNT bundles are tightly embedded in tungsten oxide.

To investigate the mechanical properties of the grown composite, tensile and shear stress-strain curves were obtained that are shown in Fig. 4(f). From these tests, the tensile strength of the composite was determined to be approximately 53 MPa with Yong's modulus of 8.79GPa. The elongation-to-break is up to 0.6% for the composite. The shear strength between the composite and the tungsten tip is approximately 3.68 MPa, which is a measure of bonding strength between the tungsten tip and the

composite. These mechanical properties are comparable to those of the macroscopic one-dimensional CNT structures fabricated by the usual methods[21-26]. It should be noted, however, that the CNTs in those studies were multi-walled long tubes whereas CNTs in this study are single-walled short tubes (<5 μm).

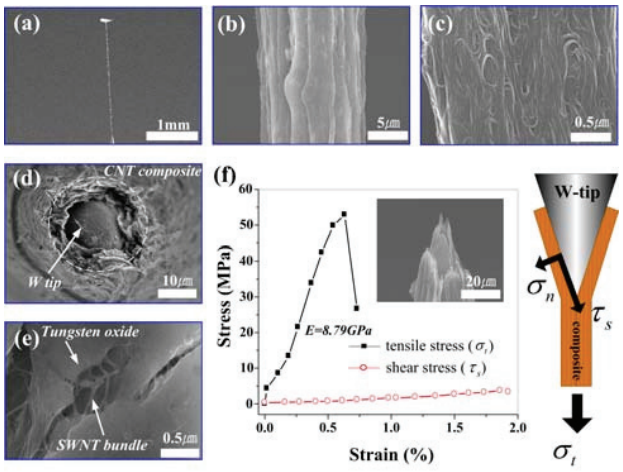

Figure 3. a) SEM(scanning electron microscopy) image of whole feature of WO_4/CNT composite structure. b) cylindrical shape (diameter: 14μm) of the composite. c) magnified SEM micrograph of well-aligned SWNT bundles along the axis of the composite. d) cross-section of the fractured composite. e) morphology of SWNT bundles mixed in tungsten oxide as revealed by the inside of delaminated composite. f) stress-strain curves of the composite. The inset shows the SEM image of the side view of the fractured composite. The schematic illustrates the tensile stress that is divided into two component forces, normal stress and shear stress.

The composition of the one-dimensional CNT structure is of interest. For the purpose, electron probe micro analysis (EPMA) technique was used to measure the atomic content of various components in the structure. The results in Fig. 4(a,b) show that as the electroplating current for fabricating the composite increases, the atomic ratio of carbon slightly decreases while that of oxygen and tungsten slightly increases. Note in this regard that sodium content is negligibly small, the ratio being less than 0.02%. Sodium in the electroplating solution is positively charged, and therefore, it is repelled by the positive potential applied to the tungsten tip. An EPMA mapping image for the distribution of tungsten component in Fig. 4(c), where red dots indicate high concentration of tungsten, shows that tungsten is well distributed all throughout the one-dimensional structure. The fact that the atomic ratio of tungsten is less than 1% is a strong indication that the structure is packed very densely with CNTs, only a small amount of tungsten oxide providing the matrix.

The electrical conductivity of the composite was also measured at room temperature. The measurements yield the conductivity of 3.12×10^2 S/cm for the pure CNT that was synthesized from CNT colloidal solution in the absence of STD and without the applied bias [28]. The samples 4 and 5 that were prepared by the crystal-like growth of the composite yield the conductivity of 1.34×10^3 S/cm and 2.14×10^3 S/cm, respectively, which are comparable to the values reported earlier for CNT fibers [30-31]. However, it is significantly higher than that for the CNT fiber fabricated using a polymer [29].

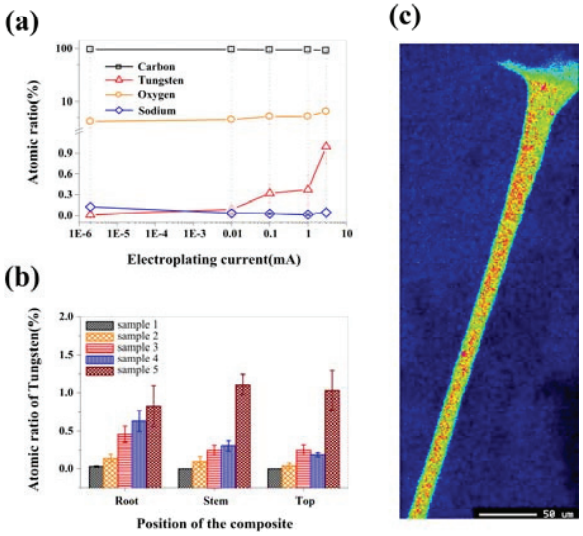

Figure 4. a) Quantitative analysis of all elements of WO_4/CNT composite as determined by electron probe micro analysis (EPMA) given as a function of electroplating current. b) tungsten atomic ratio at different positions of the composite for 5 samples. c) EPMA mapped image showing the distribution of tungsten (red dots) in the whole composite.

4. CONCLUSIONS

In summary, we have utilized non-aqueous electrolyte in place of the usual aqueous electrolyte in growing macroscopic one-dimensional metal oxide/CNT composite. Carbon nanotubes are well dispersed in the non-aqueous solution, which typically agglomerate in aqueous electrolyte without surfactants. Growing a "seed" structure initially on the electrode by electroplating and then pulling up the electrode with the bias on results in a metal oxide/CNT composite that is excellent both in mechanical and electrical properties. It has been found that CNTs are well aligned in the direction of growth or along the composite axis. The diameter of the macroscopic one-dimensional CNT composite can be manipulated by adjusting the electroplating current. The length of the structure simply increases with increasing pulling time. Although the tungsten oxide/CNT structure has CNTs interwoven in tungsten oxide, it is of interest that the atomic ratio of carbon in the structure is larger than 92%. The tungsten oxide/CNT composite is an excellent candidate for high performance point-type field emitter. Moreover, the

excellent mechanical and electrical properties of the composite should prove to be quite useful for other applications as in thermal interface material, super capacitor, and interconnects in ultra-large scale integrated circuits.

REFERENCES

[1] A. A. Mamedov, N. A. Kotov, M. Prato, D. M. Guldi, J. P. Wichsted, A. Hirsch, *Nat. Mater.* 2002, 1, 190.
[2] E. T. Thostenson, Z. Ren, T-W. Chou, *Compos. Sci. Technol.* 2001, 61, 1899.
[3] J. N. Coleman, U. Khan, Y. K. Gun'ko, *Adv. Mater.* 2006, 18, 689.
[4] S. V. Ahir, E. M. Terentjev, *Nat. Mater.* 2005, 4, 491.
[5] N. P. Padture, *Adv. Mater.* 2009, 21, 1767.
[6] C. He, N. Zhao, C. Shi, X. Du, J. Li, H. Li, and Q. Cui, *Adv. Mater.* 2007, 19, 1128.
[7] S. I. Cha, K. T. Kim, S. N. Arshad, C. B. Mo, and S. H. Hong, *Adv. Mater.* 2005, 17, 1377.
[8] Y. J. Jeong, S. I. Cha, K. T. Kim, K. H. Lee, C. B. Mo, and S. H. Hong, *Small* 2007, 3, 840.
[9] K. T. Kim, J. Eckert, S. B. Menzel, T. Gemming, and S. H. Hong, *Appl. Phys. Lett.* 2008, 92, 121901.
[10] Y. Cho, G. Choi, and D. Kim, *Electrochemical and Solid-State Letters* 2006, 9, G107.
[11] S. M. Lyth, f. Oyeleye, and R. J. Curry, *J. Vac. Sci, Technol. B* 2006, 24, 1362.
[12] H. Kang, S. Lee, and H. Lee, *J. Vac. Sci. Technol. B* 2005, 23, 563.
[13] S. Arai, M. Endo, T. Sato, and A. Koide, *Electrochemical and Solid-State Letters* 2006, 9, C131.
[14] X. H. Chen, F. Q. Cheng, S. L. Li, L. P. Zhou, D. Y. Li, *Surface and Coatings Technology* 2002, 155, 274.
[15] S. Arai, M. Endo, N. Kaneko, *Carbon* 2004, 42, 641.
[16] I. H. Kim, J. H. Kim, B. W. Cho, Y. H. Lee, and K. B. Kim, *J. Electro. Soc.* 2006, 153, A989.
[17] K. X. He, Q. F. Wu, X. G. Zhang, and X. L. Wang, *J. Electro. Soc.* 2006, 153, A1568.
[18] I. H. Kim, J. H. Kim, B. W. Cho, Y. H. Lee, and K. B. Kim, *J. Electro. Soc.* 2006, 152, A2170.
[19] P. Liu, D. Xu, Z. Li, B. Zhao, E. S. Kong, Y. Zhang, *Microelectronic Engineering* 2008, 85, 1984.
[20] W. J. Zulehner, *J. Crystal Growth* 1983, 65,189.
[21] M. Zhang, K. R. Atkinson, R. H. Baughman, *Science* 2004, 306, 1358.
[22] X. Zhang, K. Jiang, C. Feng, P. Liu, L. Zhang, J. Kong, T. Zhang, Q. Li, and S. Fan, *Adv. Mater*. 2006, 18, 1505.
[23] L. Ci, N. Punbusayakul, J. Wei, R. Vajtai, S. Talapatra, P. M. Ajayan, *Adv. Mater.* 2007, 19, 1719.
[24] Y. Wei, K. Jiang, L. Liu, Z. Chen, and S. Fan, *Nano Letters* 2007, 7, 3792.
[25] H. H. Gommans, J. W. Alldredge, H. Tashiro, J. Park, J. Magnuson, and A. G. Rinzler, *J. Appl. Phys* 2000, 88, 2509.
[26] E. Y. Jang, T. J. Kang, H. Im, S. J. Baek, S. Kim, D. H. Jeong, Y. W. Park, and Y. H. Kim, *Adv. Mater.* 2009, 21, 4357.
[27] B. Vigolo, A. Penicaud, C. Coulon, C. Sauder, R. Pailler, C. Journet, P. Bernier, P. Poulin, *Science* 2000, 209, 1331
[28] H. W. Zhu, C. L. Xu, D. H. Wu, B. Q. Wei, R. Vajtal, P. M. Ajayan, *Science* 2002, 296, 884.
[29] Y. L. Li, I. A. Kinloch, Alan H. Windle, *Science* 2004, 304, 276.
[30] L. M. Ericson, H. Fan, H. Peng, V. A. Davis, W. Zhou, J. Sulpizio, Y. Wang, R. Booker, J. Vavro, C. Guthy, A. N. G. Parra-Vasquez, M. J. Kim, S. Ramesh, R. K. Saini, C. Kittrell, G. Lavin, H. Schmidt, W. W. Adams, W. E. Billups, M. Pasquali, W. F. Hwang, R. H. Hauge, J. E. Ficher, R. E. Smalley, *Science* 2004, 305, 1447.
[31] W. Zhou, J. Vavro, C. Guthy, K. I. Winey, and J. E. Fischer, *J. Appl. Phys.* 2004, 95, 649.